# Critical Specimen Sizes for Tensile-Shear Testing of Steel Sheets

*Strength measurement of spot welds depends on both weld quality and testing specimens*

**BY M. ZHOU, S. J. HU AND H. ZHANG**

ABSTRACT. Tensile-shear testing results are influenced not only by the quality of spot welds, but also by the dimensions of testing specimens. Experimental and numerical studies have been conducted on determining critical sizes for tensile-shear testing of resistance spot welded specimens. Statistical methods have been employed, from planning stages to the analysis of results, for the purposes of getting generic relationships between the critical dimensions and the geometric variables and material properties of testing specimens. The specimen width was found the most influential, and quantitative relations were developed for testing spot welded specimens of various gauges and strengths. The systematic research results obtained in this study can be used as a guideline for tensile-shear testing specimen preparation and for analyzing testing results.

## Introduction

Strength testing is an important aspect of a weldability study in resistance spot welding (RSW), a dominant joining method in automobile body assembly. Among all tests, static tensile-shear testing is the most common laboratory test used in the determination of weld strength because of its simplicity. A comparison of specifications and recommendations by various industries and professional organizations (Ref. 1) showed significant differences in weld quality in terms of nugget size and strength requirements. The main reason for this, besides such differences in quality perception, is that there are no well-defined and accepted procedures for testing and specimen preparation.

A survey of standards and specifications reveals significant differences in testing specimen sizes for tensile-shear tests, as in almost any category of testing. As illustrated in Fig. 1, both width and length of tensile-shear testing specimens vary dramatically in practice among professional organizations. To make the difference obvious, specific dimensions are marked on a testing specimen of 0.8-mm-gauge steel — Fig. 2. Plotted in this figure are specimen size recommendations of the American National Standards Institute (ANSI) and American Welding Society (AWS, Ref. 2), the military (Ref. 3) and the International Organization for Standardization (Ref. 4). A significant difference is shown in overlap and width, with not such a drastic variance in specimen length. The width required by ISO is 45 mm, which is more than twice of that by ANSI/AWS (19 mm). Similar differences can be seen in specimen sizes of aluminum alloys. In general, there is not as much information available for testing and specimen sizes for aluminum alloys as there is for steel, primarily because of a smaller-scale application of aluminum in the automotive industry. It is found that with few exceptions the overlap of the specimens is the same as the width. The variance in specimen length is far less than that in width.

Intuitively, strength measurement of a welded specimen depends on the whole weldment, including the weld, its surroundings and the rest of the specimen (base metal). Therefore, specimens with similar welds, but with different specimen sizes or weld locations, may yield different strength measurements. Testing welded joints depends on the specimen size (width, overlap, thickness and length) and the spot weld (quality, size and location). The influence of the spot weld is often ignored in specimen size studies, and it doesn't appear in any currently available standards and specifications. The importance of testing specimen size has been recognized by several researchers. Testing specimen length was found not to be critical beyond a certain value (6 in. according to Ref. 5). The same paper also found that an overlap of equal size to the specimen width is sufficient, and the specimen width must be greater than two times the spot weld diameter to avoid pronounced reduction in the measured strength. Measured tensile-shear strength usually increases with sheet thickness, as demonstrated in a plain carbon steel by Heuschkel (Ref. 6) and in an HSLA steel by Pollard (Ref. 7), usually with increased weld diameter made with the increase in thickness. In an effort to establish rational static and dynamic tests for resistance spot welded

**KEY WORDS**

Spot Welding
Tensile-Shear Test
Resistance Welding
Nugget Size
Finite Element Model
Weld Integrity

*M. ZHOU, S. J. HU and H. ZHANG are with the Department of Mechanical Engineering and Applied Mechanics, The University of Michigan, Ann Arbor, Mich.*

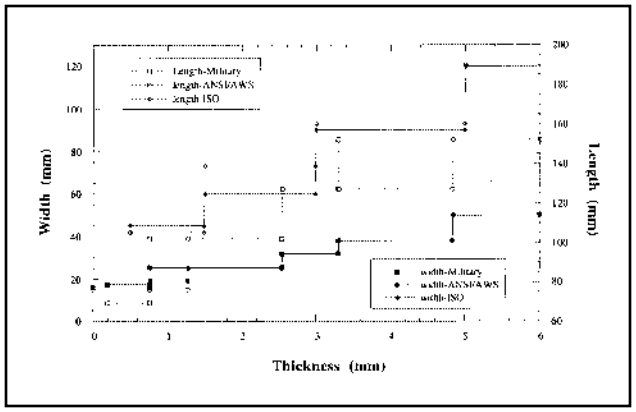


*Fig. 1 — Recommendations on width and length of tensile-shear specimens for steel sheets.*

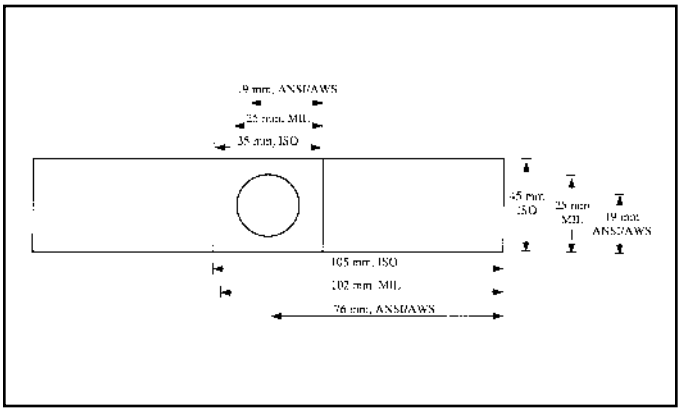


*Fig. 2 — Specimen size requirements for tensile-shear tests of 0.8-mm-gauge steel sheets.*

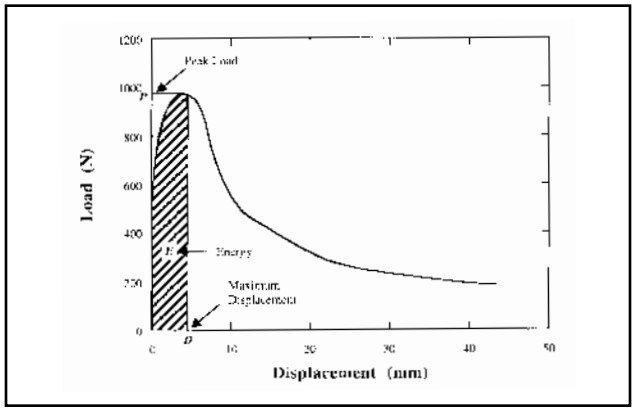


*Fig. 3 — A typical load vs. displacement curve in tensile shear testing, and definitions of variables monitored.*

low-carbon steel and high-strength steel, a series of tests was conducted in the early 1980s (Ref. 8). The effects of specimen width and overlap were the primary interests in tensile-shear testing of single welds on several gauges of steel with various mechanical properties. Overlap was found to be less critical than specimen width. A conclusion drawn from the work was that the dimensions recommended by the International Institute of Welding (IIW) are sufficiently conservative to justify their use. This work is the most up-to-date study on the specimen size sensitivity. Although it tried to learn the influence of more than one factor, it didn't provide a systematic knowledge of the effects of each individual factor, or of the interactions among these factors. Besides experimental determination, optimal specimen sizes can also be approximated through analytical analysis. The work by Koenigsberger (Ref. 9) provides useful information on quantitatively understanding the interaction between a spot weld joint and the base metal. However, because of the limitations of its closed form solutions, they do not reflect local deformation around the nugget, or consider the strength of the weld nugget. Therefore, such formulas are difficult to be used to determine optimal specimen sizes, and neglecting the shape of the nugget and local deformation tend to generate too conservative specimen dimensions.

In this study, experimental, computational and statistical studies have been conducted on the critical specimen sizes for tensile-shear testing spot welding of steels. Geometric factors, such as various dimensions, and mechanical properties of the testing specimens were studied according to their influence on the strength measurement. The objective of this study was to find the optimal sizes of tensile-shear testing specimens that are able to 1) test the quality of the weld, not the base metal; and 2) produce consistent testing results.

## Experiments

To understand the role of each dimensional variable and the interaction of the factors in affecting the measurement of tensile-shear testing, an experiment was conducted using design of experiment (DOE).

### Experiment Setup

The material used was a galvanized DS (drawing steel). Five highly influential factors (sheet thickness, length, width, overlap and weld diameter) were chosen for the experiments. For the purpose of evaluating current standards, specimen dimensions in the experiments were chosen according to ANSI/AWS and ISO (Refs. 2, 4), which represent extremes in the specimen size specifications. The dimensions were as follows (the original source is indicated in parentheses):

Thickness — 0.8 mm, 1.2 mm and 1.5 mm

Length — 76 mm (ANSI/AWS for 0.8–1.2 mm gauge steel), 105 mm (ISO for 0.8–1.2 mm gauge steel), 138 mm (ISO for 1.5 mm gauge steel)

Width — 19 mm (ANSI/AWS 0.8–1.2 mm gauge steel), 45 mm (ISO for 0.8–1.2 mm gauge steel), 60 mm (ISO for 1.5 mm gauge steel)

Overlap — 19 mm (ANSI/AWS for 0.8–1.2 mm gauge steel), 35 mm (ISO for 0.8-1.2 mm gauge steel), 45 mm (ISO for 1.5 mm gauge steel)

Weld Diameter — 4 mm and 8 mm.

Weld diameters were determined based on the formula $d = a\sqrt{t}$, similar to the relationship mentioned in the book by Koenigsberger (Ref. 9), where d is the weld diameter, t is the thickness and a is a constant that is in the range between 3 and 6. For 0.8-mm-gauge sheets, d = 3.13 mm if a is chosen to be 3.5. d = 7.35 mm for t = 1.5 mm and a = 6. So d = 4 and 8 mm were chosen to represent extreme cases. All other variables (thickness, length, width and overlap) had three levels. It is costly to conduct a full factorial design experiment for the chosen variables because of the large number of runs ($2 \times 3^4 = 162$). Besides, the influence of the variables is not the same; some are less important than others. In particular, the effects of higher-order interactions are usually insignificant. For these reasons, an orthogonal array design was adopted, which was expected to

produce results with reasonable accuracy at a significantly reduced cost. The design of experiment (DOE, $L_{36}(2 \times 3^4)$) required 36 runs, and eight replications were made on all runs.

A welding fixture was made to produce consistent and accurate samples with desired alignment, overlap and weld location. To eliminate the effects of uncontrollable factors and noise, welding and testing sequences were randomized. Welding parameters were selected to produce strong welds with designed sizes. A calibrated MTS testing machine was used for tensile-shear testing. The pulling speed was 10 mm/min, and load, displacement and failure modes were recorded.

#### Experimental Result Analysis

The most commonly monitored variable in tensile-shear testing is the peak load. In this experiment, the displacement at the peak load (maximum displacement) and the corresponding energy were also monitored, in addition to the peak load. The maximum displacement indicates the ductility, and the energy is related to the energy-absorbing capacity of the weldment. Figure 3 shows a typical load vs. displacement curve of a tensile-shear test, and the definitions of terms used in the analysis. The displacement and energy were calculated only to the peak load because the failure of specimens is basically determined at such a moment. After the load reaches its peak value, the displacement and energy are not unique because of the uncertainty in tearing the specimens.

Five types of failure (failure modes), as exhibited in the ISO standards (Ref. 4), were observed while tensile testing the specimens. The failure modes, together with corresponding characteristic load vs. displacement curves generated in the experiments are shown in Fig. 4. After reviewing the testing results, it was found that Mode A is not desirable because it only tests the base metal, as shown in Fig. 4A in which the load vs. displacement curve is very close to a typical uniform tensile testing curve. Mode B is not desirable, either. The specimen fails partly through the periphery of the weld, and partly through the base metal. Experimental results showed two similar welds on specimens with different widths result in different strength measurements when the specimens fail in Mode B. The reason is that the load-bearing capacity is influenced by the width of the base metal on the sides of the weld. In general, failure Modes A and B are observed when the testing specimen is too narrow. These two modes are not desired in weld quality testing because a quantitative measurement of weld strength cannot be obtained. Failure Modes C, D and E correspond to weld button pullout, tearing of base metal and interfacial failure. In any of these three, the quality of the welds, rather than the base metal, is tested. Therefore, failure modes serve as an indicator to whether a specimen size is proper.

Figure 5 shows failure mode maps for nominal welds of 4- and 8-mm diameters. A comparison of failure modes of specimens clearly shows how the specimen fails depends on the weld diameter, which had not been explicitly mentioned in any available specifications. Most of the samples with small welds failed in Mode E, *i.e.*, interfacial failure. Only the narrowest specimens of the thinnest gauge (0.8 mm) produced tests with failure Mode B. More A-and B-type failures were observed in the specimens with 8-mm welds. Based on the experimental observations and the above discussion, failure modes can be divided into two groups: undesirable failure modes (Modes A and B), and desirable failure modes (Modes C, D and E). This classification takes into consideration the influence on the measurement of a weld's quality by its strength and the constraint imposed by its surroundings. From Fig. 5 it can be seen that the width of 19 mm is not adequate for all three gauges, while 45- and 60-mm-wide specimens show mixed Modes C, D and E.

The experimental results were then grouped into desirable and undesirable failure modes, and they were analyzed statistically. The probability of getting desirable failure modes was predicted by a logistic regression, following the same procedure used in a study of expulsion limits (Ref. 10). It is described by the following equation:

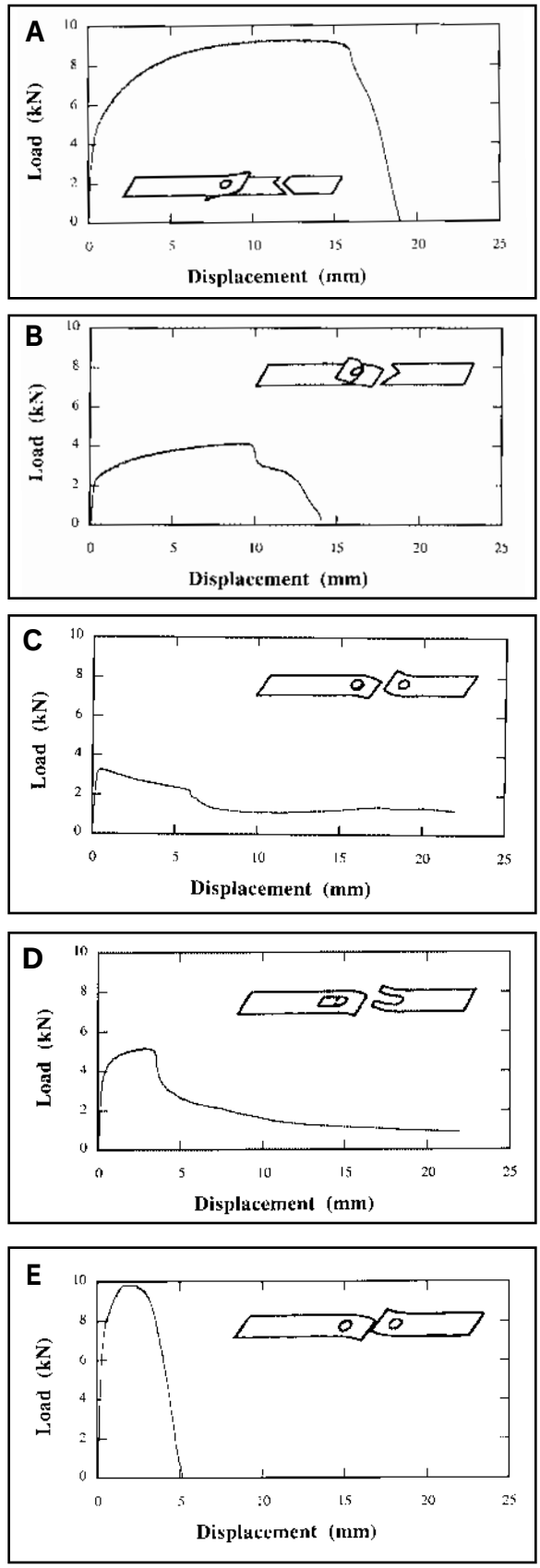


*Fig. 4 — Typical load vs. displacement curves with their corresponding failure modes in tensile-shear testing.*

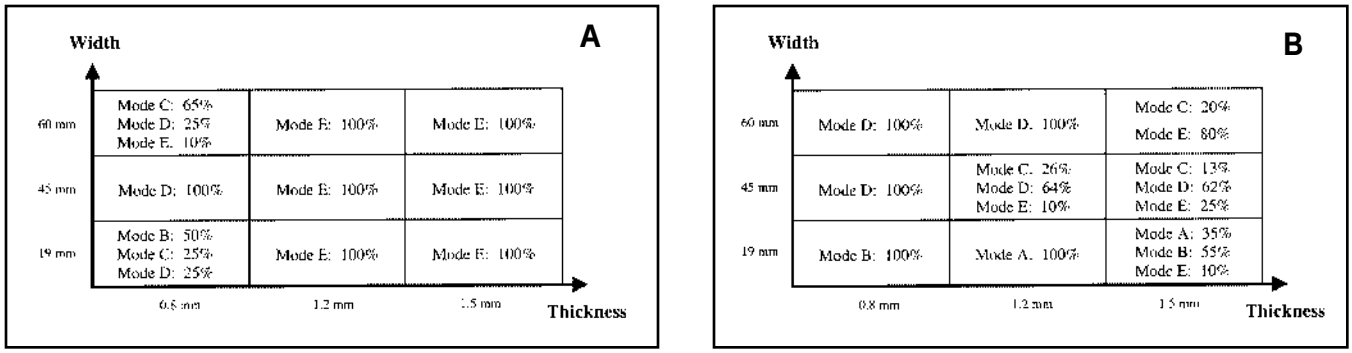


*Fig. 5 — Maps of failure modes for nominal weld diameters. A — 4 mm; B — 8 mm.*

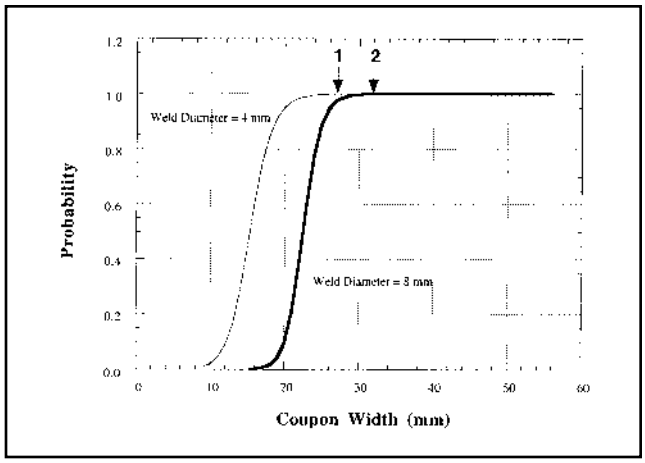


*Fig. 6 — Probability of getting desirable failure modes. Marks 1 and 2 indicate the (minimum) widths to achieve desirable failure modes for welds with 4- and 8-mm diameters.*

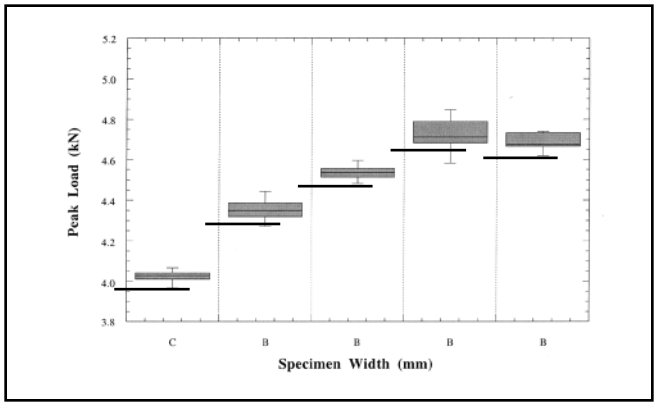


*Fig. 7 — Peak load vs. specimen width for 0.8-mm drawing steel (DS).*

$$1n\frac{P}{1-P} = a_0 + a_1 d + a_2 w_1 + a_3 w_2 + a_4 d w_1 + a_5 d w_2 \quad (1)$$

where P is the probability of getting desirable failure modes, d the linear effect of weld diameter, $w_1$ linear effect of specimen width, and $w_2$ quadratic effect of specimen width. The $a_i$s are coefficients determined from the experimental results, and they are $a_0$ = 8.673026, $a_1$ = –1.321001, $a_2$ = 9.638809, $a_3$ = –5.555071, $a_4$ = 2.800171 and $a_5$ = –1.642712.

For fixed weld diameters (4 and 8 mm), the probabilities of getting desirable failure modes are plotted as a function of specimen width in Fig. 6. Marks 1 and 2 indicate the critical widths for avoiding undesirable failure modes (A and B). The difference between the critical values is about 5 mm. The critical values are far less than those recommended by ISO. For example, 45 mm is recommended for 0.8-mm sheets and 60 mm is for 1.5-mm sheets by ISO. The critical value shown here, regardless of thickness, is 30 mm for specimens with 8-mm-diameter welds. The critical values determined in such a way are not necessarily good enough for testing weld quality. Even if a desirable failure mode is achieved, the specimen may not be wide enough to avoid excessive bending, as the sever distortion may not be confined to the vicinity of a weld.

Another way to determine critical specimen sizes is to analyze the influence of dimensional variables on strength measurements (peak load, maximum displacement and energy). Experimental results show that the thickness of specimens and weld diameter influence the peak load the most. The peak load also depends on the overlap of the specimens to some extent. Although the peak load index is often the only one used, it is not sufficient to describe the weld quality. High peak load measured on brittle/cold welds is often misleading because it may have very small ductility and, therefore, small energy-absorbing capacity. In this experiment, the maximum displacement and energy were also monitored. The specimen width is found to be far more influential than other variables on the maximum displacement. The weld diameter and the interaction between specimen width and weld diameter also strongly affect the maximum displacement. Weld diameter is the most influential on the energy absorbed by the weld, followed by the influences of width, interaction between weld diameter and width, and interaction between length and width.

Based on the above experimental and statistical studies and considering all three strength measurements (peak load, maximum displacement and energy) as a whole, four conclusions can be drawn.

1) The specimen width is the most influential dimension in tensile-shear testing.

2) The overlap is less critical and can be made the same as the width for convenience.

3) The specimen length is less influential, but it should be long enough to avoid its influence on testing. One hun-

dred fifty mm was found sufficient (25 mm was used for clamping the specimens during testing), which is longer than those found in all standards and specifications.

4) The weld diameter should be considered for different gauges of materials in determining critical specimen sizes.

The specimen width, as the most critical dimension, can be determined by plotting the strength measurements against the width. The width at which a strength measurement shifts from sharp change (with large slope) to smoother change (with small slope) was used in this study as the critical width.

Although the experiments and analysis provide important information and a methodology on the determination of critical specimen sizes, the actual values of critical width cannot be obtained accurately by doing experiments alone. The main reason for this is the inconsistency in the experimental results. For example, the peak load doesn't always stay in a plateau after the initial transition stage in Fig. 7, and the variation of measurement at each width also changes. Any variance in specimen dimension, welding and testing will influence the consistency of testing results to some extent. To overcome this problem, a finite element analysis (FEA) was conducted.

## Finite Element Simulation

Finite element simulation is a powerful tool for stress-strain analysis. For critical specimen size study, using this method avoids the uncertainty of experiments and reduces costs. Finite element modeling has not been used in the study of specimen size sensitivity in the past. Most works of finite element simulation of resistance spot welding did not differentiate material properties of the nugget and the heat-affected zone (HAZ) from the base metal. A separate study by the authors (Ref. 11) showed the dimension and mechanical properties of the HAZ significantly affect the overall performance of the welded specimens. Therefore, it is necessary to use different material properties for the nugget, the HAZ and the base metal.

In this study, a finite element model was built to simulate the behavior of spot welded specimens with the consideration of material and dimensional differences in the nugget, the HAZ and the base metal. The relationship between hardness and other mechanical properties of a weldment was established, and a numerical experiment was conducted using a statistical design of experiment.

### Finite Element Modeling

Based on the experimental results, the width is the most influential factor and the length is the least. Therefore, the finite element model used a fixed length of 150 mm for testing specimens, and the width was taken as a variable. The overlap was the same as the width. Two sheets had the same thickness. The finite element analysis was performed using a commercial software (Ref. 12). Details of the modeling can be found in the paper by Zhang, *et al.* (Ref. 11).

In the simulation, a weldment was divided into a nugget, HAZ and the surrounding base metal. As shown in Fig. 8, they have different microstructures and, therefore, different mechanical properties. These zones were distinguished from each other in the simulation. The model was created in a way that the sizes of these zones can be easily changed.

### Material Property Estimation

The various zones in a weldment are distinguished by their mechanical properties in the finite element model. However, it is difficult to test material properties of the nugget and HAZ directly. This is because the structures and properties of the nugget and the HAZ change rapidly with space, and it is impossible to prepare standard mechanical testing specimens of the nugget and the HAZ. However, mechanical properties of the weldment can be obtained indirectly through

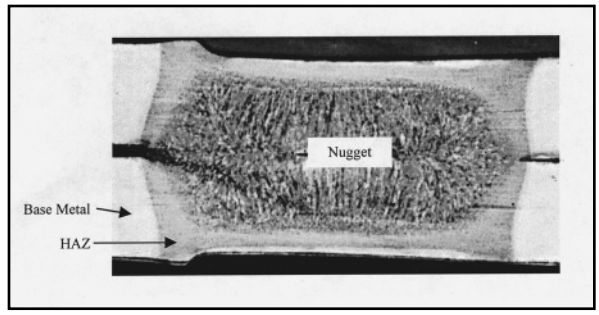


*Fig. 8 — Weld structure of a high-strength low-alloy (HSLA) steel.*

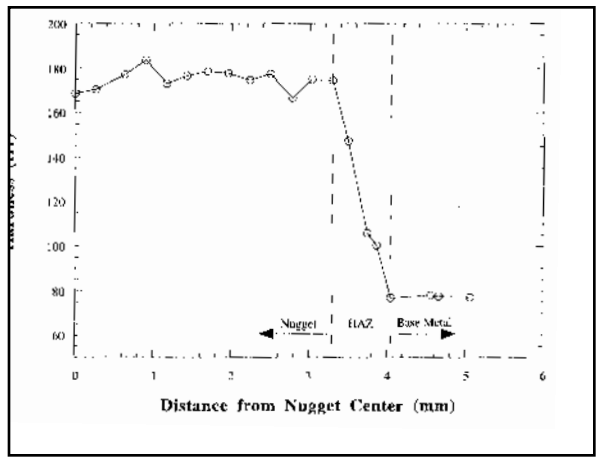


*Fig. 9 — A hardness profile of a spot weldment of a drawing steel (DS).*

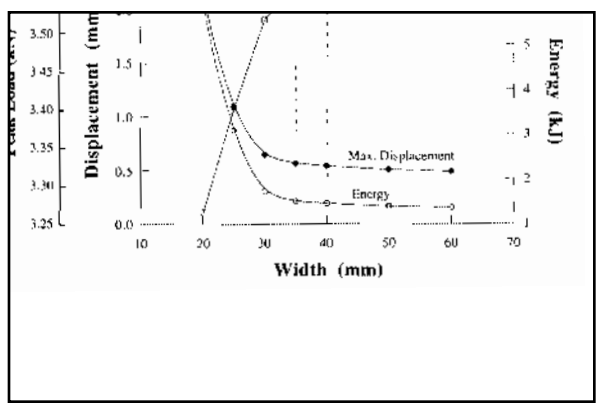


*Fig. 10 — Typical simulation results for determining critical specimen width.*

**Table 1 — Ranges Selected for Computer Simulation**

| $t$ (mm) | $h$ (mm) | $E$ (GPa) | $\sigma_y$ (MPa) | $\sigma_0$ (MPa) | $e$ (%) | $k$ |
|---|---|---|---|---|---|---|
| 0.5 ~ 2.0 | 0.1 ~ 1.5 | 190 ~ 200 | 205 ~ 1725 | 50 ~ 200 | 2 ~ 65 | 1.0 ~ 3.0 |

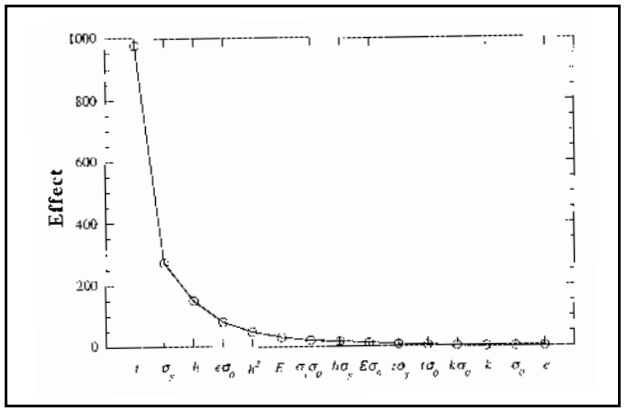


*Fig. 11 — Effects of various parameters and their interactions on the critical specimen width. Parameters shown here are in a normalized space.*

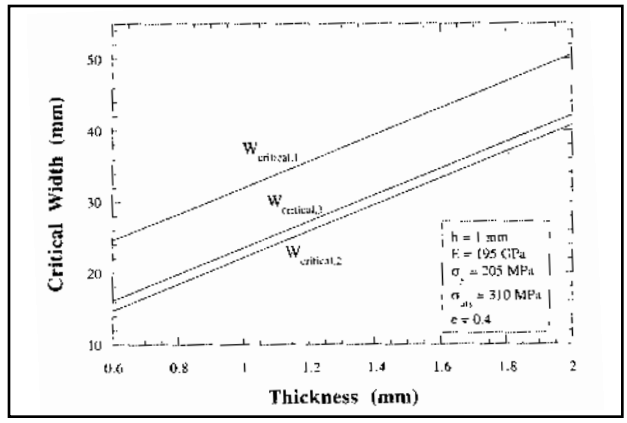


*Fig. 12 — Critical width changes with thickness for a drawing steel (DS).*

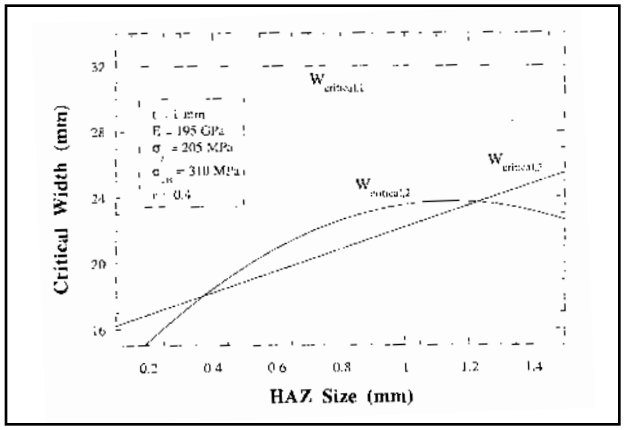


*Fig. 13 — Critical width changes with HAZ size for a DS.*

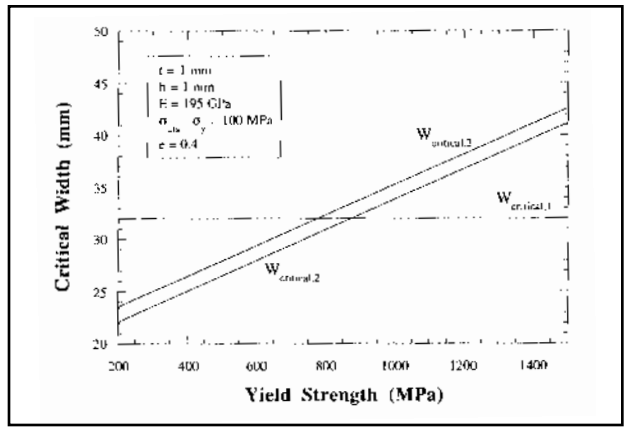


*Fig. 14 — Critical width changes with yield strength for a DS.*

empirical relationships between material strength and hardness.

There are a few works using such a relationship in welding research, or devoted to researching such relationships. For example, Satoh, *et al*. (Ref. 13), suggested a material model in their FEA analysis. By linearly varying the yield strength (based on hardness profiles) across the weld nugget and HAZ, they were able to show a strain concentration in the base metal in the low cycle loading regime that could not be predicted by a homogeneous model.

The book by Kalpakjian (Ref. 14) shows a linear relationship between hardness and yield strength. The relationship proposed is

$$\text{Hardness} = c\,\sigma_y \qquad (2)$$

where $\sigma_y$ is the yield strength and $c$ is a constant.

Zuniga and Sheppard (Ref. 15) performed experiments on a zinc-coated HSLA steel by using simulated HAZ material samples, and suggested the following relationship for the zinc-coated HSLA:

$$\sigma_y = -14.7 + 2.568\,H\nu \text{ (MPa)} \qquad (3)$$

$$\sigma_{uts} = 65.8 + 2.563\,H\nu \text{ (MPa)} \qquad (4)$$

where $\sigma_{uts}$ is the ultimate strength, and $H\nu$ is Vickers hardness. Equations 3 and 4 also indicate that $\sigma_y$ and $\sigma_{uts}$ are almost parallel because the coefficients of $H\nu$ in two equations are very close to each other.

Bourges, *et al*. (Ref. 16), proposed a correlation between hardness and tensile properties (Equations 5–7). A linear relationship is clearly shown in these equations, except in a very small correction of a quadratic term. Moreover, a link between elongation and hardness is established.

$$\sigma_{uts} = 19.13 \times 10^{-4}\,(H\nu)^2 + 1.89\,H\nu + 181.5 \text{ (MPa)} \qquad (5)$$

$$\sigma_y = \sigma_{uts} + 30.41 \log VR - 215.8 \text{ (MPa)} \qquad (6)$$

$$e = -1.38 + 18.2 \times 10^3 / \sigma_{uts} \text{ (\%)} \qquad (7)$$

where VR is cooling rate, and $e$ is ductility (elongation).

Based upon these works, the following relationships between the hardness and tensile properties were assumed for the simulation of critical specimen sizes:

$$\sigma_{uts} = \sigma_0 + k_1 * H\nu \qquad (8)$$

$$\sigma_y = k_1 * H\nu \qquad (9)$$

$$e = k_2 / H\nu \qquad (10)$$

where $\sigma_0$ is a constant, and $k_1$ and $k_2$ are proportional constants. For a spot weldment, the hardness changes continuously from the nugget, through the HAZ, to the base metal. Figure 9 shows a hardness distribution from the nugget center to the base metal. It can be seen from this

figure that the hardness can be considered constant in the nugget. In the HAZ, a linear relationship can be assumed. Thus, the hardness in the nugget can be expressed as

$$Hv = k^{*}Hv_{base} \quad (11)$$

where $k$ is a constant and $Hv_{base}$ is the hardness of the base metal. The hardness values of various zones can be related to the hardness of the base metal through Equation 11. Therefore, mechanical properties of the HAZ and the nugget can be obtained once those of the base metal are known.

#### Numerical Experiments

The purpose of this work is to find a generic relationship between the critical specimen width and the weldment geometry, as well as material properties. Figure 10 shows typical simulation results for determining critical widths. From this plot, the critical value is obtained when the curves reach the stages of slow change after a sharp transition. To determine one critical specimen width, several models of various widths are needed with same other dimensions and mechanical properties.

To obtain results with a relatively large range of application, both geometric and material properties need to vary in certain ranges. Geometric factors include the thickness ($t$) and HAZ size ($h$). The nugget diameter was taken as $6\sqrt{t}$ to overcome possible variations in size and location of the weld in real experiments. The material properties are Young's modulus ($E$), yield strength ($\sigma_y$), ultimate tensile strength ($\sigma_{uts}$), elongation ($e$) and the hardness ratio between the nugget and the base metal ($k$). The properties in the HAZ were interpolated from the nugget to the base metal.

Therefore, the critical specimen width ($W_{critical}$) can be expressed as a function of geometric variables ($t$, $h$), mechanical properties ($E$, $\sigma_y$, $\sigma_{uts}$, $e$) and the hardness ratio ($k$). Young's modulus $E$ was assumed the same for the nugget, the HAZ and the base metal. Yield strengths and elongation of the nugget and the HAZ can be derived from those of the base metal by Equations 9–11. Ultimate tensile strengths of the weldment can be similarly related to that of the base metal. Because of the relationships shown in Equations 8 and 9, only two of the three variables, $\sigma_y$, $\sigma_{uts}$ and $\sigma_0$, are needed. $\sigma y$ and $\sigma_0$ were chosen for the simulation. Therefore, the critical width can be written as

$$W_{critical} = f(t, h; E, \sigma_y, \sigma_0, e; k). \quad (12)$$

Because of the large number of variables in the function, the concept of design of experiment was employed to obtain this relationship. In this study, one run consists of obtaining a critical width (through several calculations) for a set of fixed geometric and property variables. For conventional design of experiment, a two-level full factorial design requires $2^7$=128 runs. Because at least five widths are needed for calculating one critical specimen width, there will be 640 runs total, which requires extensive computation time.

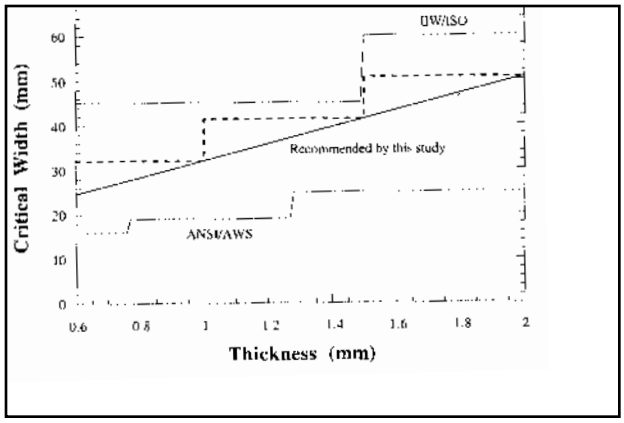


*Fig. 15 — A comparison of specimen widths calculated by this study and specified in the standards. The dashed line is the proposed specimen width.*

Rather than using a conventional full factorial design, a new statistical design specially developed for computer simulation was used in this study (Ref. 17). There are three steps in the computer simulation design. First, the number of runs ($N$) needs to be determined in the simulation based on the number of variables ($n$), then the ranges of all the variables are equally divided into $N$ levels. This is different from a conventional DOE design, which usually has very few levels (mostly two or three), and a certain number of replications of experiments is needed and decided after the number of levels and the effects to be explored are determined. Because there are no random factors in computer simulations, no replication is needed in any runs. Table 1 shows the ranges of the selected variables. After the levels and intervals are determined, the $N$ runs need to be uniformly distributed in the n-dimensional space constructed by all n variables. In

**Table 2 — Design Matrix and Simulation Results**

| Run | $v_1$ | $t$ (mm) | $v_2$ | $h$ (mm) | $v_3$ | $E$ (MPa) | $v_4$ | $k$ | $v_5$ | $\sigma_y$ (MPa) | $v_6$ | $e$ (%) | $v_7$ | $\sigma_{uts}$ (MPa) | $W_{critical}$ (mm) |
|---|---|---|---|---|---|---|---|---|---|---|---|---|---|---|---|
| 1 | 1 | 0.54 | 10 | 0.88 | 12 | 196.76 | 14 | 2.59 | 5 | 607.35 | 2 | 11 | 15 | 785.29 | 22.6 |
| 2 | 4 | 0.81 | 5 | 0.47 | 2 | 190.88 | 1 | 1.06 | 8 | 875.59 | 6 | 25 | 7 | 982.94 | 27.5 |
| 3 | 3 | 0.72 | 12 | 1.05 | 8 | 194.41 | 11 | 2.24 | 16 | 1590.88 | 5 | 22 | 1 | 1645.29 | 37.3 |
| 4 | 7 | 1.07 | 2 | 0.22 | 13 | 197.35 | 3 | 1.29 | 12 | 1233.24 | 8 | 32 | 14 | 1402.36 | 31.7 |
| 5 | 8 | 1.16 | 1 | 0.14 | 15 | 198.53 | 13 | 2.47 | 14 | 1412.06 | 11 | 42 | 6 | 1510.59 | 33.8 |
| 6 | 5 | 0.90 | 14 | 1.21 | 7 | 193.82 | 8 | 1.88 | 17 | 1680.29 | 15 | 56 | 16 | 1867.05 | 38.7 |
| 7 | 2 | 0.63 | 11 | 0.96 | 14 | 197.94 | 6 | 1.65 | 3 | 428.53 | 17 | 63 | 5 | 518.24 | 19.1 |
| 8 | 6 | 0.99 | 3 | 0.31 | 1 | 190.29 | 16 | 2.82 | 7 | 786.18 | 14 | 53 | 10 | 920.00 | 27.1 |
| 9 | 9 | 1.25 | 9 | 0.80 | 9 | 195.00 | 9 | 2.00 | 9 | 965.00 | 9 | 35 | 9 | 1090.00 | 40.4 |
| 10 | 12 | 1.51 | 15 | 1.29 | 17 | 199.71 | 2 | 1.18 | 11 | 1143.82 | 4 | 18 | 8 | 1260.00 | 44.1 |
| 11 | 16 | 1.87 | 7 | 0.64 | 4 | 192.06 | 12 | 2.35 | 15 | 1501.47 | 1 | 8 | 13 | 1661.76 | 58.2 |
| 12 | 13 | 1.60 | 4 | 0.39 | 11 | 196.18 | 10 | 2.12 | 1 | 249.71 | 3 | 15 | 2 | 312.95 | 24.2 |
| 13 | 10 | 1.34 | 17 | 1.46 | 3 | 191.47 | 5 | 1.53 | 4 | 517.94 | 7 | 29 | 12 | 669.41 | 35.7 |
| 14 | 11 | 1.43 | 16 | 1.38 | 5 | 192.65 | 15 | 2.71 | 6 | 696.76 | 10 | 39 | 4 | 777.64 | 39.2 |
| 15 | 15 | 1.78 | 6 | 0.55 | 10 | 195.59 | 7 | 1.76 | 2 | 339.12 | 13 | 49 | 17 | 534.71 | 35.0 |
| 16 | 14 | 1.69 | 13 | 1.13 | 16 | 199.12 | 17 | 2.94 | 10 | 1054.41 | 12 | 46 | 11 | 1197.06 | 49.6 |
| 17 | 17 | 1.96 | 8 | 0.72 | 6 | 193.24 | 4 | 1.41 | 13 | 1322.65 | 16 | 60 | 3 | 1394.71 | 58.9 |

Note: Columns $v_1$ to $v_7$ show designed levels.

this work, 17 runs were chosen for seven variables. The distribution of the runs were determined randomly by a computer program. Table 2 shows the values of the variables (and their corresponding levels in the design matrix) for each run. The computer simulation results are also shown in Table 2, and they were analyzed using the Kriging regression method (Refs. 18, 19).

## Results and Analysis

The dependence of critical widths on geometric variables and material properties was obtained statistically, based on the results shown in Table 2.

Figure 11 displays the effects of the variables and their interactions on the critical width. The main effects of the variables include $t$, $h$, $E$, $\sigma_y$, $\sigma_0$, $e$ and $k$. The quadratic and interaction terms of the main effects are $h^2$, $e \cdot \sigma_{032}$, $\sigma_y \cdot \sigma_0$, $h \cdot \sigma_y$, $E \cdot \sigma_0$, $t \cdot \sigma_y$, $t \cdot \sigma_0$ and $k \cdot \sigma_0$. These effects were chosen through a model selection procedure. From Fig. 11 it can be seen that thickness is extremely influential on the specimen width and its influence is about three times larger than that of the second effect ($\sigma_y$, yield strength). The HAZ size ($h$) was also found to be very important in the determination of the critical width. Other effects such as the interactions, elongation, Young's modulus, ultimate strength, etc., have much less influence on the critical width. It is interesting to notice that the hardness difference between the nugget and the base metal plays an insignificant role.

The statistical analysis yielded a few formulas for the critical widths. As shown in Fig. 11, the thickness has the largest effect on critical widths, and a function that contains only the thickness as a variable has the following form:

$$W_{critical,1} = 13.4044613 + 18.5987839\,t. \quad (12)$$

The statistical analysis revealed 53% of the total variation of critical width can be explained by this equation. If the second and third largest effects are also included, the formula is

$$W_{critical,2} = -6.0291481 + 18.5839362t + 0.0146654\sigma_y + 6.6251147h. \quad (13)$$

The variation ratio increases to 92.7% for Equation 13. If all of the first six largest effects of Fig. 11 (after transformed into the real scale) are included, the critical width is

$$W_{critical,3} = 45.6391799 + 18.5849834t + 0.0146654\sigma_y + 21.8791238h + 28.3945601e + 0.0811080\,(\sigma_{uts} - \sigma_y) - 0.0003401E - 9.5332611h^2 - 0.2280655e\,(\sigma_{uts} - \sigma_y). \quad (14)$$

For Equation 14, 98.6% of the total variation can be explained. In Equations 12, 13 and 14, units of the variables are as shown in Table 1, and the critical widths ($W_{critical,1}$, $W_{critical,2}$, $W_{critical,3}$) are in mm.

Assuming material properties for a DS — $E$ = 195 GPa, $\sigma_y$ = 205 MPa, $\sigma_{uts}$ = 310 MPa, $e$ = 40% and $h$ = 1.0 mm — critical widths can be calculated using Equations 12 through 14.

For $t$ = 0.8 mm, $W_{critical,1}$ = 28 mm, $W_{critical,2}$ = 19 mm, $W_{critical,3}$ = 20 mm.

For $t$ = 1.2 mm, $W_{critical,1}$ = 36 mm, $W_{critical,2}$ = 26 mm, $W_{critical,3}$ = 27 mm.

For $t$ = 1.8 mm, $W_{critical,1}$ = 49 mm, $W_{critical,2}$ = 37 mm, $W_{critical,3}$ = 38 mm.

To understand the influence of individual variables, the results are presented in Figs. 12–14, for the dependence of critical width on the thickness, the HAZ size and yield strength, respectively. The critical width changes linearly with the thickness in all three models — Fig. 12. The slopes are the same, while there is a shift in value. The widths predicted by Equation 12 are the greatest among all three models. The models have different responses to changes in the HAZ size — Fig. 13. Because the first model always predicts the largest critical width when the HAZ size varies, it is not necessary to use the other two models in such cases. Therefore, it is not necessary to know the HAZ size, or it can be assumed as constant. While the first model does not depend on the yield strength, the other two models have linear dependence of critical width on the yield strength — Fig. 14. When the yield strength is below 700 MPa, the first model predicts the largest critical width, and the third model gives the largest value for yield strengths above 700 MPa. This indicates the regions in which the models should be applied. For mild steel, the widths predicted by the first model should be sufficient, while the third model may work better for ultra-high-strength steel.

The critical specimen widths calculated by this study are between those specified by ANSI/AWS and ISO (Refs. 2, 4), as shown in Fig. 15. For the convenience of practical use, a step function is proposed (shown as dashed lines). It is also worth noting that although the dimensions proposed by this study are the minimum widths, they should work fairly well in most cases because they were determined using conservative values, *e.g.*, a nugget size of $6\sqrt{t}$ was used, which is rarely exceeded in practice. Therefore, there is no need to use specimens of excessive sizes.

## Summary

This study provides a systematic understanding of the influence of specimen sizes on testing results and proposes critical values for practical use. The major achievements and findings of this work can be summarized as follows:

1) Failure modes observed during tensile-shear testing provide a direct indication on the adequacy of specimen sizes. Although getting desirable failure modes is not equivalent to the suitability of specimen sizes, getting undesirable failure modes certainly means that the testing specimens are not wide enough.

2) The width is the most important factor in influencing testing measurement. It is sufficient if the overlap is the same as the width. A length of 150 mm was determined to be enough for all possible widths.

3) Numerical simulations provide consistent critical specimen widths without the influence of noise factors unavoidable in experimental studies. Statistically planned and analyzed numerical simulations make it easy at relatively low cost to obtain critical dimensions for a wide range of materials.

4) The linear dependence of critical width on the specimen thickness is found to be sufficient for determining specimen sizes for mild steels, while the more complicated yield-strength-dependent relationship is needed for high-strength steel. The quantitative relations obtained in this study are valid only for steel sheets with properties in the specified ranges. Separate research should be conducted for materials not covered by the ranges of this study.

*Acknowledgments*

The authors are grateful for the financial support of the Intelligent Resistance Welding Consortium, an Advanced Technology Program sponsored by NIST/DOC. The help provided by J. Grasse in experiments and by Dr. S. Cheng in statistical analysis are also greatly appreciated.

*References*

1. Hu, S. J., Senkara, J., and Zhang, H. 1996. Quality definition of resistance spot welds: A structural point of view, *Proc. of IBEC'96 Body & Engineering*, Detroit, Mich., pp. 91–98.

2. *Specification for Resistance Welding of Coated and Uncoated Carbon and Low Alloy Steels*, ANSI/AWS C1.4, American Welding Society, Miami, Fla.

3. *Military Specification—Welding, Resistance: Spot and Seam*, MIL-W-6858D, 1992.

4. *Specimen Dimensions and Procedure*

*for Shear Testing Resistance Spot and Embossed Projection Welds*. 1994. International Standard, ISO/DIS 14273.

5. Sparagen, W., and Cordovi, M. A. 1944. Mechanical characteristics of resistance welds in plain carbon steels. *Welding Journal* 23(7): 305-s to 343-s.

6. Heuschkel, J. 1947. Some metallurgical aspects of carbon steel spot welding, *Welding Journal* 26(10): 560-s to 582-s.

7. Pollard, B. 1974. Spot welding characteristics of HSLA steel for automotive applications. *Welding Journal* 53(8): 343-s to 350-s.

8. Rivett, R. M. 1982. Final contract report: resistance spot welding of steel sheet (for the European Coal and Steel Community). The Welding Institute, Report 3570/7/81.

9. Koenigsberger, F. 1948. *Design for Welding in Mechanical Engineering*, Longmans, Gree, and Co., pp. 81–91.

10. Zhang, H., Hu, S. J., Senkara, J., and Cheng, S. 1998. A statistical analysis of expulsion in resistance spot welding, submitted to *ASME Journal of Manufacturing Science and Engineering*.

11. Zhang, H., Zhou, M., Hu, S. J., and Senkara, J. 1999. Influence of weld attributes on spot weld tensile-shear strength, submitted to *Welding Journal*.

12. *ABAQUS* (Version 5.7) at the University of Michigan, under academic license from Hibbitt, Karlsson & Sorensen, Inc., Pawtucket, R.I.

13. Satoh, T., Abe, H., Nishikawa, K., and Morita, M. 1991. On three-dimensional elastic-plastic stress analysis of spot-welded joint under tensile shear load, *Transactions of the Japan Welding Society* 22(1): 46–51.

14. Kalpakjian, S. 1997. *Manufacturing Processes for Engineering Materials*, Addison-Wesley.

15. Zuniga, S., M., and Sheppard, S. D. 1995. Determining the constitutive properties of the heat-affected zone in a resistance spot weld, *Modelling & Simulation In Materials Science & Engineering* 3(3):391–416.

16. Bourges, P. H., Jubin, L., and Bocquet, P. 1995. Prediction of mechanical properties of weld metal based on some metallurgical assumptions. *Mathematical Modelling of Weld Phenomena*, ed. H. Cerjak, Institute of Materials, London, pp. 201–212.

17. Koehler, J. R., and Owen, A. B. 1996. *Computer Experiments, Design and Analysis of Experiments*, North-Holland, Amsterdam, pp. 261–308.

18. Matheron, G. 1963. Principles of geostatics. *Econom. Geol*. 58:1246–1266.

19. Gressie, N. 1986. Kriging nonstationary data. *Journal of the American Statistical Association* 81: 625–634.

## Preparation of Manuscripts for Submission to the *Welding Journal* Research Supplement

All authors should address themselves to the following questions when writing papers for submission to the Welding Research Supplement:

- ◆ Why was the work done?
- ◆ What was done?
- ◆ What was found?
- ◆ What is the significance of your results?
- ◆ What are your most important conclusions?

With those questions in mind, most authors can logically organize their material along the following lines, using suitable headings and subheadings to divide the paper.

1) **Abstract.** A concise summary of the major elements of the presentation, not exceeding 200 words, to help the reader decide if the information is for him or her.

2) **Introduction.** A short statement giving relevant background, purpose and scope to help orient the reader. Do not duplicate the abstract.

3) **Experimental Procedure, Materials, Equipment.**

4) **Results, Discussion.** The facts or data obtained and their evaluation.

5) **Conclusion.** An evaluation and interpretation of your results. Most often, this is what the readers remember.

6) **Acknowledgment, References and Appendix.**

Keep in mind that proper use of terms, abbreviations and symbols are important considerations in processing a manuscript for publication. For welding terminology, the *Welding Journal* adheres to ANSI/AWS A3.0-94, *Standard Welding Terms and Definitions.*

Papers submitted for consideration in the Welding Research Supplement are required to undergo Peer Review before acceptance for publication. Submit an original and one copy (double-spaced, with 1-in. margins on 8 ½ x 11-in. or A4 paper) of the manuscript. Submit the abstract only on a computer disk. The preferred format is from any Macintosh® word processor on a 3.5-in. double- or high-density disk. Other acceptable formats include ASCII text, Windows™ or DOS. A manuscript submission form should accompany the manuscript.

Tables and figures should be separate from the manuscript copy, and only high-quality figures will be published. Figures should be original line art or glossy photos. Special instructions are required if figures are submitted by electronic means. To receive complete instructions and the manuscript submission form, please contact the Peer Review Coordinator, Doreen Kubish, at (305) 443-9353, ext. 275; FAX 305-443-7404; or write to the American Welding Society, 550 NW LeJeune Rd., Miami, FL 33126.